Friction stir welding of glass fiber-reinforced polyamide 6: Analysis of the tensile strength and fiber length distribution of friction stir welded PA6-GF30

Article *in* IOP Conference Series Materials Science and Engineering · March 2019

DOI: 10.1088/1757-899X/480/1/012013

CITATION
1

READS
214

4 authors, including:

Benedict Jaeger
Technische Universität München
1 PUBLICATION **1** CITATION

SEE PROFILE

Friction stir welding of glass fiber-reinforced polyamide 6: Analysis of the tensile strength and fiber length distribution of friction stir welded PA6-GF30

IOP Conf. Series: Materials Science and Engineering 480 (2019) 012013 doi:10.1088/1757-899X/480/1/012013

Friction stir welding of glass fiber-reinforced polyamide 6: Analysis of the tensile strength and fiber length distribution of friction stir welded PA6-GF30

S P Meyer*, B Jaeger, C Wunderling and M F Zaeh

Institute for Machine Tools and Industrial Management (iwb), Technical University of Munich, Boltzmannstr. 15, 85748 Garching, Germany

* e-mail: stefan.meyer@iwb.mw.tum.de

Abstract. Friction stir welding (FSW) is a solid state welding process that is preferably used for aluminum alloys. In the study described here, FSW was applied to glass fiber-reinforced polyamide 6 (PA 6) and evaluated in terms of weld strength and fiber length distribution in the weld seam. For this purpose, the main effects on the tensile strength for friction stir welded specimens with a stationary shoulder were investigated. It could be shown that small tilt angles in combination with high contact pressures are advantageous. Using the optimum settings, a tensile strength of 50% of the base material strength could be achieved. Furthermore, an optical measuring method for large-volume fiber length measurement is introduced and evaluated. It has been demonstrated that the fibers shorten during the process. However, this has only a minor influence on the strength, while the influence of the tilt angle, the contact pressure, and the feed rate are significant.

1. Introduction

Friction stir welding (FSW) is a solid state joining technology and was patented in December 1991 by "The Welding Institute" (TWI) [1]. The main application is the joining of aluminum alloys, which are difficult to weld by using conventional fusion welding processes like laser beam welding [2]. Since FSW only softens and stirs the material, but does not melt it, high-strength compounds can be produced [3]. Due to this advantage, FSW is often used in sectors with a focus on lightweight constructions such as the aerospace or the automotive industry [3].

For lightweight construction plastics are also being used to an increasing extent. Fiber-reinforced plastics in particular offer the possibility to achieve high specific strengths with low densities. [4] However, joining fiber-reinforced plastics is still a challenge [5]. One problem is that during conventional welding processes (e.g. heating element welding) the fibers align parallel to the seam. This leads to reduced strength and introduces weak spot. [5–8]

Since the material flow in the process zone during FSW is different from conventional welding methods, it is assumed, that joining fiber-reinforced plastics using FSW increases the weld line strength due to an adapted reorientation of the fibers in the seam.

The aim of this work is to investigate the influence of different process and tool parameters on the tensile strength and fiber length distribution of glass fiber-reinforced polyamide 6.

2. State of the art

2.1. Conventional welding methods for plastics

A variety of methods can be used for joining plastics. These include processes such as screwing, riveting, clipping, and adhesive bonding. However, these processes have considerable disadvantages with regard to the force propagation, which is often only possible at certain junctions. Also, additional mass is introduced through the mechanic joining elements (e.g. screws, rivets, or adhesives). These disadvantages can be avoided by welding [9]. In the following, various welding techniques for polymers will be discussed.

According to MENACHER [10], the welding processes can be classified corresponding to their heat input mechanisms. These include heat conduction (e.g. hot plate welding), convection (e.g. extrusion welding), radiation (e.g. infrared welding), friction via internal friction (e.g. ultrasonic welding), and friction by means of external friction (e.g. vibration welding and friction stir welding) [9;10] . Especially in industrial environments, hot plate welding and vibration welding are frequently employed. However, these methods have limited applicability for fiber-reinforced plastics due to a reduction of the weld strength compared to the strength of the base material [5; 7]. This relationship is defined by the welding factor *S*:

$$S = \frac{R_{m,weld}}{R_{m,base}}, \qquad (1)$$

with $R_{m,weld}$ as maximum tensile strength of the welded sample and $R_{m,base}$ as maximum tensile strength of the base material.

In hot-plate-welding, the joining partners are heated by a contact surface until the joining partners plasticize in the contact area. The joining parts are then pressed together with the plasticized ends and thereby welded. The pressure applied to the joining zone causes a so-called squeeze flow, which presses the molten plastics out of the joining zone (see Figure 1). A more detailed description of the melt flow is given in section 2.2. In addition to the contact temperature *T*, the welding parameters include the contact pressure p and the dwell time *t*. [11]

With hot-plate-welding of various fiber-reinforced polymers welding factors between 0.42 and 0.83 can be achieved. For example, for a polypropylene (PP) with 25%[1] glass fiber-reinforcement, a weld factor of 0.42 was achieved [7]; with fiber reinforcements of 30%, strengths of 0.6 [12] and 0.61 [5] could be obtained. For polyamide (PA) with 30% glass fiber-reinforcement, a composite strength of 0.5 could be reached [12]. FIEBIG & SCHOEPPNER [5] achieved a weld factor of 0.83 for PA6-GF30. Here the fiber orientation within the weld seam was also examined and compared with the initial orientation of the fibers. It was found that a high amount of fibers were aligned parallel to the joining zone. FIEBIG & SCHOEPPNER [5] explained this based on the squeeze flow and the original fiber alignment.

In vibration welding, the components are moved relative to each other. In most cases one component is stationary, while the second component is set in motion with a frequency *f* and an amplitude *A* relative to it. Due to the high speed movements under a defined contact pressure, the components heat up and plasticize at the contact surface. A sudden deceleration and actuation of pressure causes the plastic material to solidify and the components to form a joint. Similar to hot-plate-welding, the squeeze flow causes material to be distributed parallel to the joining plane. [11]

For vibration welding of fiber-reinforced plastics, welding factors between 0.14 and 0.67 were achieved [5; 7]. GEHDE et al. [7] recorded a welding factor of 0.14 to 0.23 for polypropylene (PP) with 25% glass fiber reinforcement. FIEBIG & SCHOEPPNER [5] were able to obtain a welding factor of 0.56 for a PP with 30% glass fiber reinforcement and 0.67 for polyamide (PA) with 30% glass fiber-reinforcement. FIEBIG & SCHOEPPNER [5] also pointed out that the orientation of the fibers before the

[1] All weight data refer to weight percent.

welding process has a considerable influence on the strength of the joint. The paper showed, that the highest strength could be achieved for injection-molded test specimens [5]. KAGAN [13] investigated the influence of the fiber content on the relative weld strength. He showed that the welding factor for PA decreases with increasing fiber content. For unreinforced polyamide, a welding factor of almost 1 was achieved, while for PA with 45% glass fiber content the factor was only 0.39. [13]

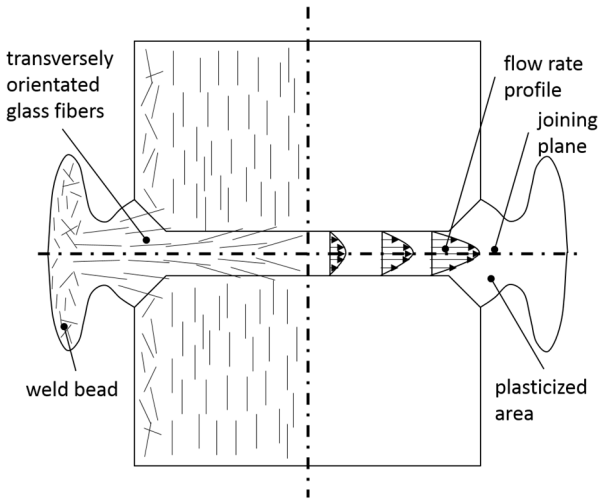

Figure 1. Schematic drawing of the reorientation of fibers in the weld zone due to the squeeze flow, based on [12].

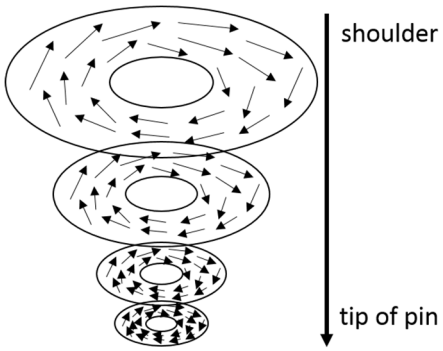

Figure 2. The vector field of the velocity around a probe is shown graphically for friction stir welding, based on [14].

2.2. Melt flow during welding

One reason for the low welding factor of fiber-reinforced plastics compared to unreinforced plastics is the fiber orientation in the weld seam [5; 15]. As a result of the squeeze flow, the fibers are aligned perpendicular to the joining direction (see Figure 1). This results in a weld seam in which the reinforcing fibers are not aligned in the loading direction.

This means that the force is not transferred by the fibers in the welding zone. Rather, the fibers weaken the joint which leads to a reduced force transmission. [5–8; 15; 16]

Compared to the described conventional welding processes, the material flow during FSW is not perpendicular to the weld [17; 14; 18], but rather the material is transported around the pin [17].

ZHANG ET AL. [19] showed a numerical approach to describe the particle distribution in the FSW process on an Al 6061-T6 alloy plate. NANDAN ET AL. [14] depicts for friction stir spot welding (FSSW) that the material rotates around the pin, where the velocity on the relative position of the pin length (see Figure 2). SIMÕNES & RODRIGUES [20] presented the theory that the various thermo-mechanical properties of plastics lead to a differing material flow in the seam. One assumption is that the fibers in fiber-reinforced plastics are distributed differently during an FSW process compared to conventional welding techniques (e.g. hot plate welding or vibration welding). This distribution could lead to increased values of the welding factors when using FSW for joining fiber-reinforced plastics.

2.3. Influence of the fiber length on the tensile strength

In addition to the fiber orientation, the fiber length has a major influence on the strength of the composite material [21; 22]. In order to take full advantage of the strength of the fibers in the reinforced polymer, the fiber length l has to be longer than the critical fiber length l_c:

$$l \geq l_c \qquad (2)$$

The critical fiber length l_c is defined by equation 3:

$$l_c = \frac{\sigma_{Fb} * d_f}{2 * \tau_b}, \quad (3)$$

with σ_{Fb} as fiber breakage resistance, d_f as fiber diameter and τ_b as shear strength of the matrix.

The critical fiber length describes the required length to transmit force through the interfaces until the complete fiber strength σ_{Fb} is reached. Thus, fibers above the critical fiber length ensure that the complete fiber strength is exploited and in the event of an overload a fiber breakage or a combination of fiber pull-out and breakage occurs. Fibers shorter than l_c cannot reach the full strength, meaning that the fiber-polymer composite does not reach the maximum possible strength. [22] During processing of discontinuous fiber-reinforced plastics, fibers are subject to thermal and mechanical stresses. These lead to fiber breakage and shortening during the process. A good overview of fiber breakage mechanisms, as well as a method for fiber length determination can be found in [21].

2.4. Friction stir welding for polymers

Friction stir welding of thermoplastic materials is currently a popular topic of research and is not yet employed in industry. In the following, the most important findings regarding FSW of polymers are discussed.

STRAND [23] investigated the FSW process for unreinforced polypropylene (PP). For this purpose, a special tool with a “hot shoe” was developed, which warms the joining zone by using a heated shoulder and thus guarantees an improved heat input. In particular, the microstructure in the weld was examined and compared with that of the base material. The typical FSW onion-like rings could be found in the plastic component as well. Furthermore, it could be shown that a large pin diameter, a low feed rate, and a high heating capacity are advantageous. [23] The “hot shoe” concept introduced by STRAND [23] was also adopted and studied by other authors [24–27]. Using this method, MOSTAFAPOUR & TAFHIZAD [26] were able to join an unreinforced PA 6 with a welding factor of 0.9.

Based on these results, AYDIN [28] investigated the effect of preheated UHMWPE (ultra high molecular weight polyethylene) samples on the weld strength. It was found that the strength increases depending on the preheating temperature, with an optimum in the range of 70 – 90°C. [28]

Fundamental studies on friction stir welding of thermoplastic materials are primarily focused on polyolefins (PE and PP) [29–31]. It was shown that the process parameters rotational speed and feed rate have the greatest influence on the strength [30].

SADEGHIAN & BESHARATI [32] investigated the influence of the pin profile on the tensile strength of friction stir welded acrylonitrile butadiene styrene (ABS). However, both the conical and the cylindrical pin showed similar results.

The influence of the axial force on the weld strength of ABS was investigated on an FSW machine [33] and on a welding robot [34]. It was found that higher axial forces reduce welding defects. The feasibility of joining polymers by FSW with a robot was proven. [33, 34]

Besides polyolefins, polyamides are a frequently used group of polymers. Therefore, PANNEERSELVAM & LENIN [35] and HUSAIN ET AL. [36] investigated this group of materials. It could be demonstrated that there is an optimal rotational speed at which the specimens reach the maximum tensile strength [36]. Furthermore, [35] showed that a threaded pin reduces the weld defect susceptibility in polyamide specimens.

It has been demonstrated that a threaded conical pin also produces the best results for fiber-reinforced plastics (PP with 30% carbon fiber) [37; 38]. CZIGÁNY & KISS [39] demonstrated that the FSW process shortens the fibers in the plastic; nevertheless, fiber bridge bonds are formed. It is suspected that shorter fibers lead to the reduced strength. However, strength could increase due to the orientation of the fibers [39].

2.5. Fiber length measurement

The fiber length measurement of short glass fibers is regulated in ISO 22314 [40]. The method is structured in the following steps:

1. Removal of the matrix via pyrolysis
2. Fiber distribution in a water bath by ultrasound
3. Manual measurement of (300±60) fibers with a microscope

However, this procedure is time-consuming. Therefore, GORIS ET AL. [21] developed an optical method based on a scanner solution and automatic image processing using a MATLAB algorithm. The first step, the removal of the matrix via pyrolysis, is executed according to the standard. Then, the fiber separation is performed by a fiber distribution system. For this purpose, the fibers are placed in a device (a type of funnel) and distributed over a glass plate using compressed air. The glass plate is then scanned and evaluated by a MATLAB algorithm. This method was shown to provide comparable results.

3. Objective and approach

The aim of the work described in this paper was to investigate the potential of FSW as a technology for joining fiber-reinforced plastics with a focus on the influence of the fiber length.

To achieve this, a process window for welding polyamide 6 with 30% glass fiber reinforcement was found. The produced specimens were tested for tensile strength and the fiber length distribution in the weld seam.

4. Experimental setup

4.1. Test rig and tools

The experiments were conducted with an industrial robot (KUKA KR500-MT) using an FSW spindle. Furthermore, a patented DeltaN tool, i.e. a tool with a stationary shoulder, was used [41]. The FSW tool, which was used throughout the experiments, consisted of a flat shoulder with a diameter of $d_{S,1}$ = 20 mm and $d_{S,2}$ = 24 mm and a conical pin (cone angle δ_{Pin} = 10°, tip diameter $\delta_{Pin,tip}$= 4.7 mm, pin length l_{Pin} = 5 mm, M8 thread).

4.2. Welding material and tensile test

The tests were conducted on polyamide 6 plates with 30% glass fiber reinforcement (trade name: TECAMID 6 GF30 black) from Ensinger GmbH. The material had a thickness of 5.3 mm. Selected properties are given in Table 1.

Table 1. Selected mechanical and thermal properties of the examined polyamide 6 with 30% glass fibers [43].

Mechanical properties			
Young´s modulus	E	5700	MPa
Tensile strength	R_m	98	MPa
Elongation	ε	4	%
Thermal properties			
Glass transition temperature	T_a	49	°C
Melting temperature	T_m	218	°C
Specific thermal capacity	c	1.3	J/(g*K)
Thermal conductivity	λ	0.41	W/(K*m)

The plastic plates were cut into 300 x 100 mm samples and welded together in butt joint configuration with a seam length of 250 mm. In accordance with DIN EN ISO 527-3 (specimen geometry 2), 20 mm wide sections were cut out and prepared for tensile testing (see Figure 3) [42]. The tensile strength R_m of the produced specimens was measured with a tensile testing machine type 'Z020' from Zwick GmbH & Co. KG.

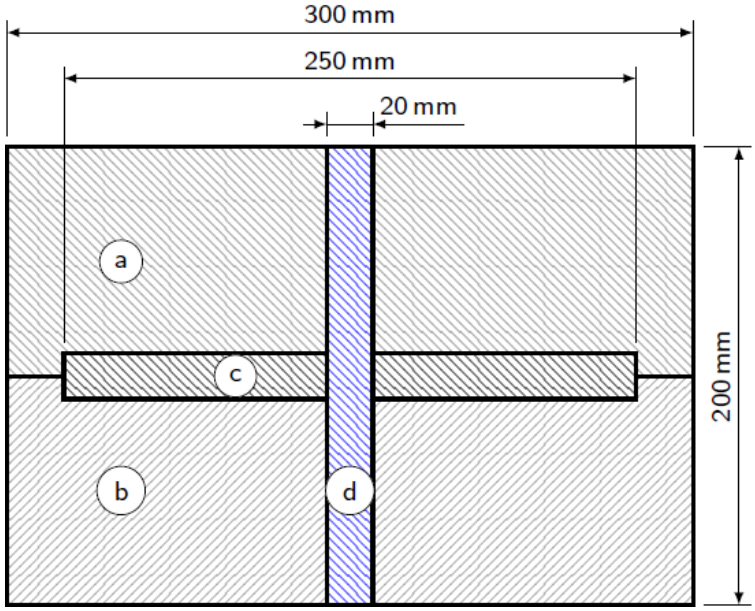

Figure 3. Schematic drawing of the joining partners (a and b) with indicated weld seam position (c) and tensile test specimen (d)

4.3. Fiber length analysis

In order to determine the fiber lengths in the weld seam, an optical measuring method was developed based on GORIS ET AL. [21] and SCHÄFER ET AL. [44] using a MATLAB algorithm. For this purpose, a 10 x 10 x 5.5 mm piece was cut out of the joining zone and ashed at (625±25) °C using a muffle furnace (model: WT-TM 18-S from WENDEL-TEC GmbH) according to DIN EN ISO 1172 [45]. The sample was held in a glow bowl and covered for the duration of the ashing (approx. 45 – 60 min) due to the risk of fire. During this process, the matrix material burned and exposed the fibers. Afterwards, the fibers were distributed on a glass plate via a fiber separation system similar to that of GORIS ET AL. [21]. For this purpose, the fibers were placed in the separation system and sputtered by compressed air. As a result, the fibers were separated and broadly distributed over the glass plate. The glass plate was then scanned in a lighting tent using a reflex camera (Canon EDS 60D) with a special close-up lens (Canon EF 50mm f/2.5 Compact Macro). To determine the magnification through the lens and to achieve the correction of the pixel length to the true length, a glass scale was placed on the glass plate during scanning. The dimensions of the high-precision glass scale were known and could therefore be used to convert the pixel length to the true length using the calibration factor k:

$$k = \frac{true\ length}{pixel\ length} \tag{4}$$

To evaluate the fiber length, the images taken were imported and evaluated using a MATLAB algorithm. First, the contrast of the image was increased using the *imadjust(x)* command (compare Figure 4a to Figure 4b). This command saturates the lower 1% and the upper 1% of all pixel values. This operation allows a better visibility of the fibers in the image. Next, the image was binarized using a global threshold method (ISO50% method) based on a gray value histogram (see Figure 4c). For this

purpose, the gray value histogram of the image was determined and two peaks were detected due to the bimodal distribution of the values. The peak with the lower gray value was defined as background, while the peak with the higher gray value was identified as fiber. Then, the threshold value TH_{global} was determined with equation 5:

$$TH_{global} = \frac{Gray{-}Value_{Material} + Gray{-}Value_{Background}}{2} \quad (5)$$

The gray scale image *g(x,y)* could then be converted with the threshold value TH_{global} into a binary image *b(x,y)*:

$$b(x,y) = \begin{cases} 0 \\ 255 \end{cases} for\ g(x,y) \begin{matrix} < TH_{global} \\ \geq TH_{global} \end{matrix} \quad (6)$$

Thereafter, filter operations were applied to detect and eliminate errors such as pixel errors, agglomerations, and edge defects in the binary image. For this purpose, a filter was applied that separates and eliminates dust grains and other artifacts below a certain size. A second filter was used, which detects and deletes agglomerated objects. The third filter discerns objects that were located on the edge and thus were probably not completely in the field of view of the camera. These particles will be ignored. The last filter operation was used to detect overlapping objects. In this context, an ellipse was placed around each detected contiguous object and the aspect ratio was determined (see Figure 4d). Oblong fibers have a small aspect ratio, while crossing fibers have a relatively high aspect ratio and can therefore be detected and ignored. Through these filter operations, an image could be generated which can be analyzed based on the fiber length. In this image, contiguous objects were detected and measured using the Pythagorean approach (see Figure 4e). Then the length was determined by using the calibration factor from equation 4 and evaluated.

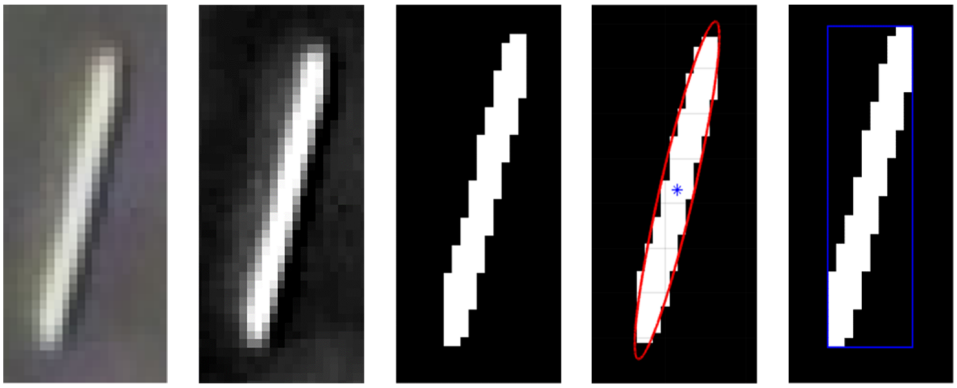

Figure 4. Exemplary detail display of a glass fiber during filter operations: (a) original gray scale image, (b) section after the contrast adjustment, (c) binary image, (d) ellipsis plot to determine the aspect ratio, and (e) length calculation by using the Pythagorean approach

5. Results and discussion

5.1. Process window

As mentioned in the state of the art, the influence of the rotational speed has already been examined in detail. For this research, the rotational speed of 1000 1/min (first plasticization of the polymer) was gradually increased. At a rotational speed of 2000 1/min a uniform plasticization of the material could be observed. At the same time, the best seam surfaces appeared here. Subsequently, the rotational speed was set to 2000 1/min and only the parameters tilt angle α, feed rate v, axial force F_z, and shoulder diameter d_S were varied (see Table 2).

Table 2. Overview of the used parameters and results of the tensile tests including the base material (BM); the standard deviation was calculated from 5 samples.

No.	Shoulder diameter d_S in mm	Rotational speed n in 1/min	Tilt angle α in °	Downward force F_Z in N	Feed rate v in mm/min	Tensile strength R_m in MPa	Standard deviation
1	20	2000	2	2000	25	49.04	4.03
2	20	2000	1	1500	40	8.61	0.91
3	20	2000	1	1500	25	28.91	14.14
4	20	2000	2	1500	25	12.05	7.09
5	20	2000	2	2000	40	11.12	2.81
6	24	2000	1	2000	25	14.83	8.06
7	24	2000	2	1500	25	16.23	6.29
8	24	2000	1	1500	10	18.82	8.70
9	24	2000	2	2000	25	10.67	4.30
10	24	2000	2	1500	25	16.59	9.10
11	24	2000	2	2000	40	8.80	2.65
12	24	2000	1	1500	25	10.01	1.70
BM	-	-	-	-	-	98	-

In order to be able to evaluate the influence of the individual parameters, a statistical experimental design was developed. Two values were tested for each of the above mentioned parameters.

5.2. Analysis of the tensile strength

Figure 5 shows the results of the tensile tests. For each value, 5 samples were evaluated. Except for samples 1 and 3, the strengths are low and the scatter of the values compared to the base material.

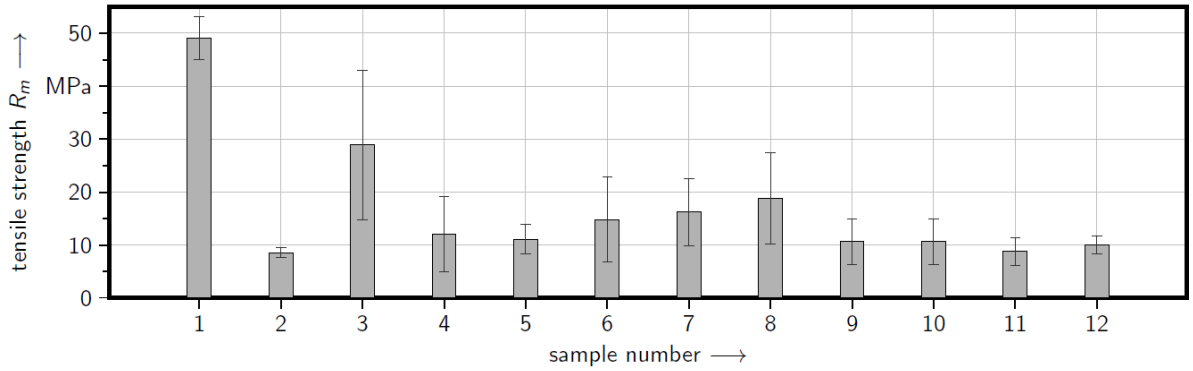

Figure 5. Bar chart of the results of the tensile tests and the corresponding standard deviation of 5 samples; the corresponding process parameters are listed in Table 2.

A statistical evaluation of the experiments shows that small shoulder diameters in combination with small tilt angles, low feed rates and high contact forces are advantageous (see Figure 6). Both smaller shoulder diameters and higher contact forces increase the contact pressure and thus the compression in the weld seam. Lower feed rates lead to an increased energy input and thus to a lower viscosity. This improves the dynamics of the material flow during the welding process. This effect can lead to fibers being carried along better and improve their orientation in the weld seam.

However, some effects seem to be contrary. A large shoulder diameter has advantages with a lower contact force and high feed rates.

The tilt angle is advantageous for low angles. This effect is independent of the contact force and the feed rate.

The influence of the shoulder diameter is significant. A comparison between sample 1 and sample 9 shows that only 1/5 of the strength is achieved, although only the shoulder diameter was varied.

The samples always broke on the retreating side.

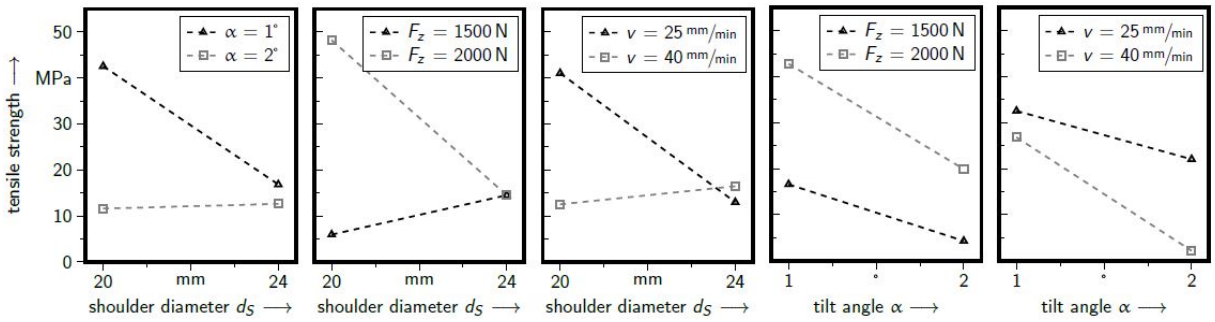

Figure 6. Statistical evaluation of the samples with regard to shoulder diameter and tilt angle.

5.3. Analysis of the cross-sections

The analysis of the cross-sections shows that the weld seam quality on the advancing side (AS) is significantly better (see Figure 7). On the retreating side (RS), shrinkage holes and pores were frequently formed. One possible reason for that could be the heat generation, which is lower on the RS. This means that the plasticized material cannot adhere to the base material at all or only with very limited adhesion. As a result, the joint is often discontinuous and the strength tends to be lower.

Comparing the micrographs of sample 1 (see Figure 7a) and sample 4 (see Figure 7b) shows that a reduced contact force F_z increases pore formation on the retreating side (RS). The effect of a higher feed rate is shown by a comparison from sample 1 to sample 5 (see Figure 7c). Besides a tunnel error in sample 5, the poor joint quality on the retreating side is visible. Additional pores can be seen on the advancing side, which further reduce the joint strength. By examining sample 1 and sample 9 (see Figure 7d), the influence of the larger shoulder diameter can be seen. A poor connection as well as a tunnel error is visible in sample 9.

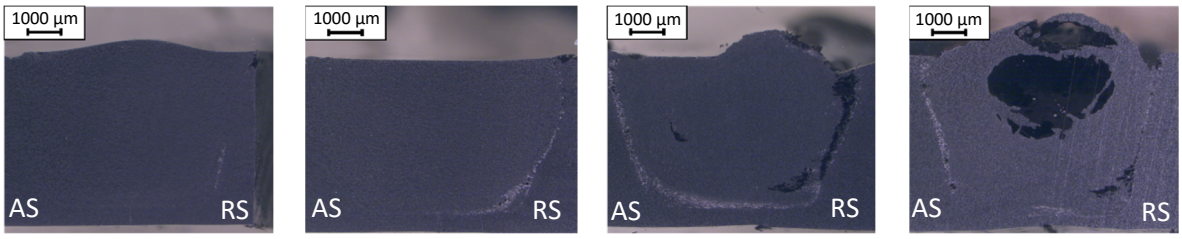

(a) sample 1 (b) sample 4 (c) sample 5 (d) sample 9

Figure 7. Micrographs of different samples with advancing side (AS) on the left side and retreating side (RS) on the right side of each cross section.

5.4. Analysis of the fiber length

The analysis of the fiber lengths of all samples shows that the fibers break during the process and shorten by 10 – 20% (see Figure 8). However, no correlation between the process parameters and the fiber shortening could be identified.

The distribution of the fiber lengths remains similar, compared to the base material. Both the base material and the welded samples show a normal distribution. The average fiber lengths are far below the critical fiber length. Fibers shorter than 0.3 mm are not detected by the measuring system due to the filter settings. Although this setting falsifies the measurement results, this adjustment is permissible as fibers smaller than 0.3 mm do not improve the strength.

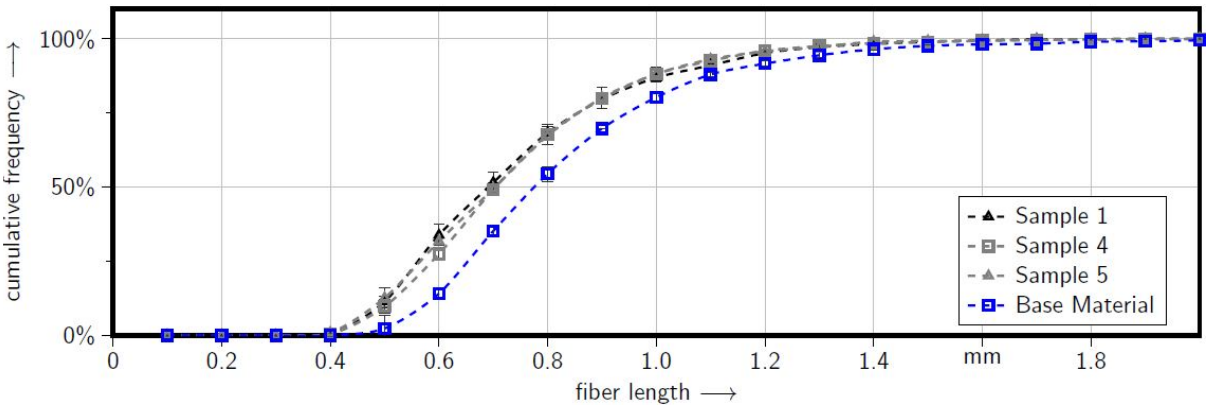

Figure 8. Comparison of the cumulated frequencies of the fiber lengths of different samples compared to the base material.

6. Conclusion and discussion

The influence of the process parameters on the joint strength of friction stir welded PA6-GF30 samples could be demonstrated in this study. It could be shown that a small tilt angle is to be preferred for FSW of plastics. Small feed rates, small shoulder diameters and high contact pressures are also advantageous. With the best parameter setting ($\alpha = 2°$, $F_z = 2000$ N, $v = 25$ mm/min and $d_S = 20$ mm) a maximum welding factor of 0.5 could be achieved. Furthermore, a method for large volume measurement of glass fibers was presented and evaluated. It could be shown that the FSW process breaks the fibers and shortens them. However, this shortening has no noticeable influence on the strength of the welded joint. This leads to the conclusion that the tensile strength is mainly influenced by the process parameters.

Thus it can be said that the process itself has to be controlled in a stable and reproducible way before the reinforcing fibres have a reinforcing effect. Furthermore, the fiber orientation in the joining zone should be investigated to check how the reinforcing fibers are deposited.

Acknowledgments

This research and development project is funded by the German Federal Ministry of Education and Research (BMBF) within the Framework Concept “Research for Tomorrow’s Production” (funding number 02P16Z010 – 02P16Z014) and managed by the Project Management Agency Karlsruhe (PTKA). The author is responsible for the contents of this publication.

References

[1] Thomas W M, Nicholas E D, Needham J C, Murch M G, Temple-Smith P and Dawes C J Improvements relating to friction welding **WO 1993 01 09 35 A1**
[2] Mishra R S and Ma Z Y 2005 Friction stir welding and processing *Materials Science and Engineering: R: Reports* **1-2** 1–78
[3] Thomas W M and Nicholas E D 1997 Friction stir welding for the transportation industries *Materials & Design* **4-6** 269–273
[4] Lyu M-Y and Choi T G 2015 Research trends in polymer materials for use in lightweight vehicles *International Journal of Precision Engineering and Manufacturing* **1** 213–220
[5] Fiebig I and Schoeppner V 2016 Influence of the Initial Fiber Orientation on the Weld Strength in Welding of Glass Fiber Reinforced Thermoplastics *International Journal of Polymer Science* 1–16
[6] Bucknall C B, Drinkwater I C and Smith G R 1980 Hot plate welding of plastics: Factors affecting weld strength *Polymer Engineering & Science* **6** 432–440
[7] Gehde M, Giese M and Ehrenstein G W 1997 Welding of thermoplastics reinforced with random glass mat *Polymer Engineering & Science* **4** 702–714

[8] Potente H, Natrop J, Pedersen T K and Uebbing M 1993 Comparative Investigations into the Welding of Glass-Fiber-Reinforced PES *Journal of Thermoplastic Composite Materials* **2** 147–159
[9] Stokes V K 1989 Joining methods for plastics and plastic composites: An overview *Polymer Engineering & Science* **19** 1310–1324
[10] Menacher M Vibrationsschweißen von strahlenvernetztem Polyamid 66
[11] Baur E, Brinkmann S, Osswald T A, Rudolph N and Schmachtenberg E 2013 Saechtling Kunststoff Taschenbuch
[12] Bruessel A 1999 Fertigungstechnische und werkstoffspezifische Aspekte zum Fügen von Thermoplasten mittels Heizelement
[13] Kagan V 2003 Optimized Mechanical Performance of Welded and Molded Butt Joints: Part I — Similarities and Differences *Journal of Reinforced Plastics and Composites* **9** 773–784
[14] Nandan R, Roy G G and Debroy T 2006 Numerical simulation of three-dimensional heat transfer and plastic flow during friction stir welding *Metallurgical and Materials Transactions A* **4** 1247–1259
[15] Kamal M R, Chung Y-M and Gomez R 2008 Three-dimensional fiber orientation in vibration welded joints of glass fiber reinforced polyamide-6 *Polymer Composites* **9** 954–963
[16] Fiebig I and Schoeppner V 2018 Factors influencing the fiber orientation in welding of fiber-reinforced thermoplastics *Welding in the World* **8** 751
[17] Seidel T U and Reynolds A P 2001 Visualization of the material flow in AA2195 friction-stir welds using a marker insert technique *Metallurgical and Materials Transactions A* **11** 2879–2884
[18] Kumar K and Kailas S V 2008 The role of friction stir welding tool on material flow and weld formation *Materials Science and Engineering: A* **1-2** 367–374
[19] Zhang H W, Zhang Z and Chen J T 2005 The finite element simulation of the friction stir welding process *Materials Science and Engineering: A* **1-2** 340–348
[20] Simões F and Rodrigues D M 2014 Material flow and thermo-mechanical conditions during Friction Stir Welding of polymers: Literature review, experimental results and empirical analysis *Materials & Design* 344–351
[21] Goris S, Back T, Yanev A, Brands D, Drummer D and Osswald T A 2017 A novel fiber length measurement technique for discontinuous fiber-reinforced composites: A comparative study with existing methods *Polymer Composites* **6**
[22] Fu S 1996 Effects of fiber length and fiber orientation distributions on the tensile strength of short-fiber-reinforced polymers *Composites Science and Technology* **10** 1179–1190
[23] Strand S Jan. 2003 Joining plastics - can friction stir welding compete? *Electrical Insulation Conference and Electrical Manufacturing and Coil Winding Conference* 321–326
[24] Bagheri A, Azdast T and Doniavi A 2013 An experimental study on mechanical properties of friction stir welded ABS sheets *Materials & Design* 402–409
[25] Mostafapour A 2012 A study on the role of processing parameters in joining polyethylene sheets via heat assisted friction stir welding: Investigating microstructure, tensile and flexural properties *International Journal of the Physical Sciences* **4**
[26] Mostafapour A and Taghizad Asad F 2016 Investigations on joining of Nylon 6 plates via novel method of heat assisted friction stir welding to find the optimum process parameters *Science and Technology of Welding and Joining* **8** 660–669
[27] Azarsa E and Mostafapour A 2014 Experimental investigation on flexural behavior of friction stir welded high density polyethylene sheets *Journal of Manufacturing Processes* **1** 149–155
[28] Aydin M 2010 Effects of Welding Parameters and Pre-Heating on the Friction Stir Welding of UHMW-Polyethylene *Polymer-Plastics Technology and Engineering* **6** 595–601
[29] Saeedy S and Givi M K B 2011 Investigation of the effects of critical process parameters of friction stir welding of polyethylene *Proceedings of the Institution of Mechanical Engineers, Part B: Journal of Engineering Manufacture* **8** 1305–1310

[30] Bozkurt Y 2012 The optimization of friction stir welding process parameters to achieve maximum tensile strength in polyethylene sheets *Materials & Design* 440–445
[31] Gao J, Shen Y, Zhang J and Xu H 2014 Submerged friction stir weld of polyethylene sheets *Journal of Applied Polymer Science* **22** n/a-n/a
[32] Sadeghian N and Besharati Givi M K 2015 Experimental optimization of the mechanical properties of friction stir welded Acrylonitrile Butadiene Styrene sheets *Materials & Design* 145–153
[33] Mendes N, Loureiro A, Martins C, Neto P and Pires J N 2014 Effect of friction stir welding parameters on morphology and strength of acrylonitrile butadiene styrene plate welds *Materials & Design* 457–464
[34] Mendes N, Loureiro A, Martins C, Neto P and Pires J N 2014 Morphology and strength of acrylonitrile butadiene styrene welds performed by robotic friction stir welding *Materials & Design* 81–90
[35] Panneerselvam K and Lenin K 2014 Joining of Nylon 6 plate by friction stir welding process using threaded pin profile *Materials & Design* 302–307
[36] Husain I M, Salim R K, Azdast T, Hasanifard S, Shishavan S S and Eungkee Lee R 2015 Mechanical properties of friction-stir-welded polyamide sheets *International Journal of Mechanical and Materials Engineering* **1** 241
[37] Ahmadi H, Arab N B M, Ghasemi F A and Farsani R E 2012 Influence of Pin Profile on Quality of Friction Stir Lap Welds in Carbon Fiber Reinforced Polypropylene Composite *International Journal of Mechanics and Applications* **3** 24–28
[38] Ahmadi H, Mostafa Arab N B and Ghasemi F A 2014 Optimization of process parameters for friction stir lap welding of carbon fibre reinforced thermoplastic composites by Taguchi method *Journal of Mechanical Science and Technology* **1** 279–284
[39] Czigány T and Kiss Z Friction stir welding of fiber reinforced polymer composites *Proceedings of the 18th International Conference on Composite Materials*
[40] Deutsches Institut für Normung e. V. DIN EN ISO **DIN EN ISO 527-3** Plastics - Determination of tensile properties
[41] Silvanus J, Forster E and Tauscher E Schweißwerkzeug zum Verbinden von wenigstens zwei Werkstücken, Schweißverfahren und Werkstück **DE 10 2011 106 506 A1**
[42] Deutsches Institut für Normung e. V. DIN EN ISO **DIN EN ISO 1172** Prepregs, Formmassen und Laminate
[43] Ensinger Ltd 20.02.2018 TECAMID 6 GF30 black - Stock Shapes
[44] Schäfer C, Meyer S P and Osswald T A 2018 A novel extrusion process for the production of polymer micropellets *Polymer Engineering & Science* 1391
[45] ISO Internationale Organisation für Normung. ISO **22314** Plastics -- Glass-fibre-reinforced products -- Determination of fibre length